Cytoplasmic dynein participates in apically targeted stimulated secretory traffic in primary rabbit lacrimal acinar epithelial cells

Yanru Wang[1], Galina Jerdeva[1], Francie A. Yarber[1], Silvia R. da Costa[1], Jiansong Xie[2], Limin Qian[2], Chadron M. Rose[2], Constance Mazurek[5], Noriyuki Kasahara[4,5], Austin K. Mircheff[2,3] and Sarah F. Hamm-Alvarez[1,2,3,*]

Departments of Pharmaceutical Sciences[1], Physiology and Biophysics[2], Ophthalmology[3], Pathology[4] and Institute for Genetic Medicine[5], University of Southern California, 1985 Zonal Avenue, Los Angeles, CA 90033, USA

*Author for correspondence (e-mail: shalvar@hsc.usc.edu)

Accepted 28 January 2003
Journal of Cell Science 116, 2051-2065 © 2003 The Company of Biologists Ltd
doi:10.1242/jcs.00398

Summary

A major function of the acinar cells of the lacrimal gland is the production and stimulated release of tear proteins into ocular surface fluid. We investigate the participation of cytoplasmic dynein in carbachol-stimulated traffic to the apical plasma membrane in primary rabbit lacrimal acinar epithelial cells. Confocal fluorescence microscopy revealed a major carbachol-induced, microtubule-dependent recruitment of cytoplasmic dynein and the dynactin complex into the subapical region. Colocalization studies, sorbitol density gradient/phase partitioning analysis and microtubule-affinity purification of membranes showed that some dynein and dynactin complex were associated with VAMP2-enriched membranes. Adenovirus-mediated overexpression of p50/dynamitin inhibited the recruitment and colocalization of dynein, the dynactin complex and VAMP2 in the subapical region. Nocodazole treatment and p50/dynamitin overexpression also depleted subapical stores of rab3D in resting acini, suggesting that dynein activity was also involved in maintenance of rab3D-enriched secretory vesicles. These data implicate cytoplasmic dynein in stimulated traffic to the apical plasma membrane in these secretory epithelial cells.

Key words: Microtubule, Exocytosis, rab3D, VAMP2, Dynein, Acinar secretion

Introduction

A major function of the acinar cells of the lacrimal gland is the production and stimulated release of tear proteins including lysosomal hydrolases and growth factors into nascent tear fluid (Fullard, 1994). Activation of DAG/Ca^{2+}-dependent pathways, mimicked in vitro by the cholinergic agonist, carbachol (CCH), or cAMP-dependent pathways can trigger the release of secretory proteins (Dartt, 1994). Although the signaling pathways are well defined, the identities of the downstream molecular effectors of stimulated tear protein secretion remain elusive.

Previous work has established that treatment with microtubule (MT)-targeted drugs reduces stimulated lacrimal acinar secretion (Robin et al., 1995; da Costa et al., 1998). However, these studies did not identify the MT-based motor protein responsible nor define the step(s) involved. Two families of MT-based motor proteins are known, the kinesins and the cytoplasmic dyneins (Hirokawa, 1998). Lacrimal acinar MTs are organized with their minus-ends beneath the apical membrane (da Costa et al., 1998), suggesting that MT-dependent traffic into this region would utilize a minus-end directed motor-like cytoplasmic dynein.

Conventional cytoplasmic dynein is a large multisubunit complex of ~1400 kDa consisting of two heavy chains (500-530 kDa) and several intermediate (DIC, 74 kDa) light/intermediate (51-61 kDa) and light (8, 14, 22 kDa) chains (Holzbaur and Vallee, 1994). Dynein heavy chain contains sites for MT binding and ATP hydrolysis, and is responsible for generation of mechanochemical force. The remaining dynein subunits may specify cargo interactions and/or regulate heavy chain function. Directed transport of vesicles by conventional cytoplasmic dynein requires a multiprotein complex called the dynactin complex (Gill et al., 1991). This complex functions as an adapter, mediating dynein binding to different cargo structures (Allan, 1996; Schroer, 1996; Holleran et al., 1998). The dynactin complex exhibits two major structural features including a 37 nm actin-like filament largely comprised of the actin-related protein, Arp1, attached to a 24 nm sidearm largely comprised of a dimer of $p150^{Glued}$ (Schafer et al., 1994). The $p150^{Glued}$ sidearm interacts with DIC (Vaughan and Vallee, 1995) and MTs (Waterman-Storer et al., 1995). p50/dynamitin, a dynactin complex protein, may mediate the interaction of $p150^{Glued}$ and the Arp1 filament (Echiverri et al., 1996). When overexpressed in mammalian cells, it is thought to prevent complex formation between the $p150^{Glued}$ sidearm and the membrane-associated Arp1 filament (Echiverri et al., 1996; Burkhardt et al., 1997). We refer to conventional cytoplasmic dynein and p50/dynamitin as dynein and dynamitin.

Here we focus on CCH-induced changes in dynein and dynactin complex association with lacrimal acinar membranes

enriched in one of two secretory vesicle markers, vesicle-associated membrane protein 2 (VAMP2) or rab3D. Originally identified on neuronal secretory vesicles, VAMP2 has been identified in acinar epithelial cells from several exocrine tissues including lacrimal gland (Fujita-Yoshigaka et al., 1996). Studies in parotid and pancreatic acini implicate VAMP2 in secretagogue-stimulated exocytosis (Gaisano et al., 1994; Fujita-Yoshigaka et al., 1996; Hansen et al., 1999). Proteins of the rab3 subfamily of small GTP-binding proteins are likewise implicated in exocytosis (Fischer von Mollard et al., 1994), with rab3D constituting the principal isoform associated with secretory vesicles in pancreas, parotid gland and lacrimal gland (Ohnishi et al., 1996; Valentijn et al., 1996).

In rabbit lacrimal acini, we show by confocal fluorescence microscopy that CCH promotes accumulation of dynein and the dynactin complex in the subapical region. Colocalization studies and biochemical analysis of isolated subcellular membranes suggest that at least one vesicle population transported towards the apical membrane by dynein is enriched in VAMP2. Adenovirus-mediated overexpression of dynamitin prevents the recruitment and colocalization of dynein, the dynactin complex and VAMP2 beneath the apical membrane. Nocodazole treatment or dynamitin overexpression also depletes subapical stores of rab3D in resting acini, suggesting that dynein may also maintain this mature secretory vesicle population at the apical membrane.

Materials and Methods

Reagents

CCH, nocodazole, rhodamine-phalloidin, LDH Activity Assay kits and goat anti-mouse secondary antibody conjugated to FITC were obtained from Sigma Chemical (St Louis, MO). Mouse monoclonal antibodies (mAbs) to dynamitin, p150^{Glued} and γ-adaptin were from Transduction Laboratories (Lexington, KY). Rabbit polyclonal antibodies to VAMP2 and rab6 were purchased from Stressgen Biotechnologies (Victoria, British Columbia, Canada) and Santa Cruz Biotechnology (Santa Cruz, CA), respectively. The 74.1 mouse mAb to DIC was obtained from Chemicon (Temecula, CA). The rabbit polyclonal antibody to rab3D and the mouse mAb to Arp1 were the generous gifts of James Jamieson (Yale University) and Trina Schroer (Johns Hopkins University), respectively. Goat anti-mouse and anti-rabbit IRDye™800-conjugated secondary antibodies were purchased from Rockland (Gilbertsville, PA). Goat anti-mouse and anti-rabbit horseradish peroxidase-conjugated secondary antibodies and ECL reagents were obtained from Amersham (Arlington Heights, IL). Matrigel was obtained from Collaborative Biochemicals (Bedford, MA). ProLong antifade mounting medium and goat anti-rabbit secondary antibody conjugated to Alexa Fluor 568 were from Molecular Probes (Eugene, OR). Cell culture reagents were from Life-Technologies. Protease inhibitor cocktail produced from Sigma reagents was used as described (Yang et al., 1999).

Cell isolation and culture

Isolation of lacrimal acini from female New Zealand white rabbits (1.8-2.2 kg) obtained from Irish Farms (Norco, CA) was in accordance with the Guiding Principles for Use of Animals in Research. Lacrimal acini were isolated as described (da Costa et al., 1998; Yang et al., 1999; Qian et al., 2002) and cultured for 2-3 days. Cells prepared in this way aggregate into acinus-like structures; individual cells within these structures display distinct apical and basolateral domains and a polarized cytoskeleton, and maintain a robust secretory response (da Costa et al., 1998).

Confocal fluorescence microscopy

For analysis of DIC, p150^{Glued} or Arp1 distribution with VAMP2, rab3D or actin filaments, acini cultured on Matrigel-coated coverslips were rinsed with Dulbecco's PBS (DPBS), fixed and permeabilized with ethanol at –20°C for 10 minutes, rehydrated in DPBS (Mendell and Whitaker, 1978) and blocked with 1% bovine serum albumin. Acini were then incubated with appropriate primary and fluorophore-conjugated secondary antibodies and/or rhodamine phalloidin. For dynamitin detection, acini were fixed in 4% paraformaldehyde, permeabilized in 0.1% Triton X-100 (Tx-100) and processed as above. Samples were imaged using a Nikon PCM Confocal System equipped with Argon ion and green HeNe lasers attached to a Nikon TE300 Quantum inverted microscope. Images were compiled in Adobe Photoshop 7.0 (Adobe Systems, Mountain View, CA).

Quantitation of western blots

For quantitation of proteins on western blots, the majority of blots were processed using secondary antibodies conjugated to IRDye™800 and quantified using an Odyssey Scanning Infrared Fluorescence Imaging System (Li-Cor, Lincoln, NE). With tubulin as standard, we have established that this system is linear over a 12-fold range (R^2=0.98); our scanned values fall within this range. For display, fluorescent signals were converted digitally to black and white. Some experiments included in summary analyses used secondary antibodies conjugated to horseradish peroxidase for ECL detection and quantitation by densitometry.

Detergent extraction

Sequential detergent extraction was as described by Hollenbeck (Hollenbeck, 1989). Lacrimal acini on Matrigel-coated dishes were exposed to extraction buffer (0.1 M PIPES, pH 7.0, 5 mM $MgSO_4$, 10 mM EGTA, 2 mM DTT supplemented with protease inhibitor cocktail) containing 4% polyethylene glycol, 10 μM taxol and 0.02% saponin for 12 minutes at 37°C. Extraction buffer supplemented with 4% polyethylene glycol, 10 μM taxol and 1% Tx-100 was then added for 8 minutes at 37°C. After rinsing, the remaining material was scraped into extraction buffer containing 1% SDS. The distribution of proteins of interest across pools was determined by SDS-PAGE and western blotting.

Subcellular fractionation analysis

Resting and CCH-stimulated acini were resuspended, lysed and analyzed by differential sedimentation and isopycnic centrifugation on hyperbolic sorbitol gradients as described (Hamm-Alvarez et al., 1997; Yang et al., 1999; Qian et al., 2002). Sedimented membrane fractions were resuspended in sorbitol cell lysis buffer and snap frozen in liquid nitrogen before storage at –80°C. Phase partitioning analyses of membranes from selected, pooled density gradient fractions were performed as described (Mircheff, 1989), concentrated by differential centrifugation and resuspended and frozen as described above. Proteins of interest were analyzed and quantified either on western blots or using activity measurements (β-hexosaminidase, alkaline phosphatase) as previously described (Mircheff, 1989). Density gradient distributions are expressed as the percentage of the total recovered in the 13 fractions, whereas phase partitioning distributions are expressed as cumulative percent recovery (Yang et al., 1999). CCH stimulation had no significant effect on the total amounts of each marker recovered in the membranes. Differences between the amount of each of the proteins in corresponding fractions from parallel CCH-stimulated and control gradients were evaluated with Student's *t*-test with $P \leq 0.05$.

MT-affinity isolation of membranes

Isolation of membranes by MT-affinity was as previously described

(Goltz et al., 1992). Briefly, supernatant containing microsomal membranes from resting and CCH-stimulated (100 μM, 15 minutes) acini were incubated with taxol-polymerized porcine brain MTs. Bound membranes were cosedimented with the MT pellet under conditions that pelleted MTs but not microsomal membranes, and attached membranes were released with excess Mg-ATP. DIC and VAMP2 contents in ATP-releasable membrane fractions from resting and stimulated acini were assessed by western blotting of equivalent amounts of total protein.

Generation of adenoviral vectors

Recombinant adenoviral (Ad) vectors were constructed using the AdEasy Vector System (Quantum Biotechnologies). Human dynamitin cDNA (provided by Janis Burkhardt, University of Chicago, with permission from Richard Vallee, University of Massachusetts) was cloned into the shuttle plasmid, pAdTrack, containing a CMV-driven green fluorescent protein (GFP) marker gene and arms of homology to the left and right ends of the Ad5 genome flanking a plasmid backbone containing the kanamycin resistance gene. Shuttle plasmids were linearized and co-electroporated into the recombinogenic *E. coli* BJ5183 strain with the 30 kb supercoiled plasmid, pAdEasy, containing the Ad genome in an ampicillin-resistant plasmid. Transformants were selected on kanamycin plates, mini-prep DNA from resistant colonies was screened by restriction digest, and clones showing the correct restriction pattern were re-transformed into *E. coli* DH10 to prevent recombination. Virus stocks were produced by transfection of recombinant Ad genomes into 293 cells, amplification and purification of harvested virus by cesium chloride ultracentrifugation. Viral titers were determined using the tissue culture infectious dose$_{50}$ assay on 293 cells. For these studies, 2-day acinar cultures were transduced at a MOI of 5 PFU/ml for 4 hours, followed by rinsing and recovery for 16-18 hours at 37°C.

Secretion assays

Transduced acini seeded in Matrigel-coated 24-well plates were incubated in fresh medium before removal of an aliquot for measurement of protein content or β-hexosaminidase activity. After treatment with or without CCH (100 μM, 30 minutes), a second aliquot of medium was removed for measurement of these values. In each assay, protein and β-hexosaminidase release were calculated from 5-6 replicate wells/treatment and normalized to total cellular protein. Differences between post- and pre-incubation values from unstimulated acini represent basal release. Differences between post- and pre-incubation values from stimulated acini represent total release (basal plus stimulated). The stimulated value was calculated by subtracting basal release from total release. Differences in experimental groups were determined using a paired *t*-test with $P \leq 0.05$. Protein was measured with the Micro-BCA Protein Assay (Pierce) using bovine serum albumin as standard, and β-hexosaminidase activity was assessed using methyumbelliferyl-β-D-glucosaminide as substrate.

Results

CCH promotes MT-dependent recruitment of dynein and dynactin to the subapical region of acini

Figs 1 and 2 show the labeling patterns associated with dynein and two constituents of the dynactin complex, p150^{Glued} and Arp1, in parallel with actin filaments in resting and CCH-stimulated lacrimal acini. Actin labeling facilitates ready identification of apical/lumenal membranes because of its enrichment at the apical cortex and within microvilli. In resting acini, dynein exhibited a diffuse labeling pattern (Fig. 1A,C). CCH stimulation resulted in a large increase in the labeling intensity of dynein beneath the apical plasma membrane (Fig. 1D,F).

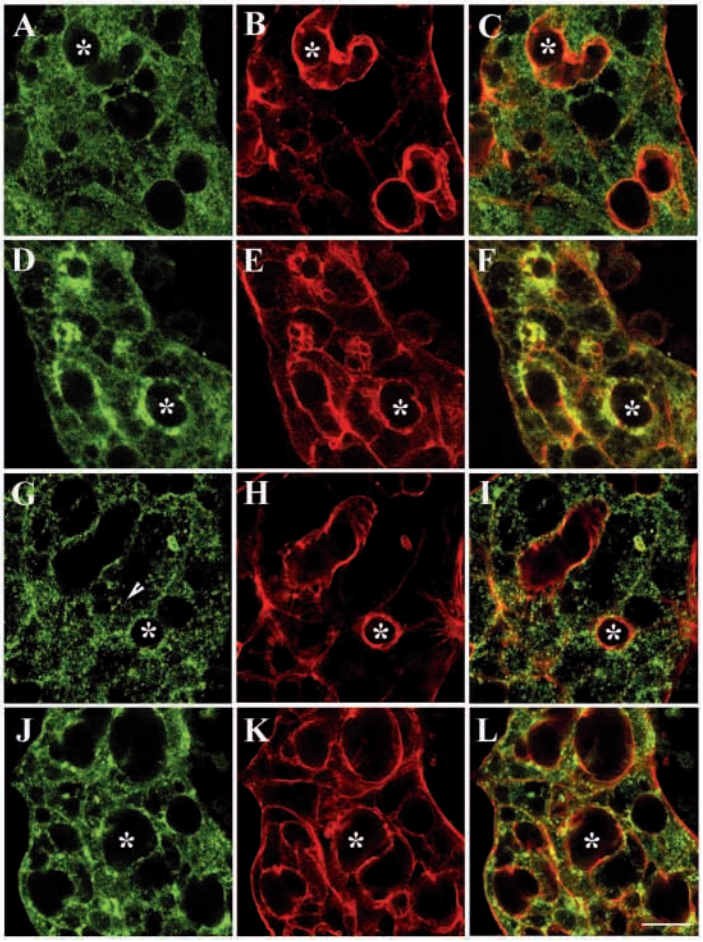

Fig. 1. CCH promotes MT-dependent recruitment of dynein to the subapical region of acini. Lacrimal acini were fixed and processed for labeling of dynein and actin filaments, and imaged by confocal fluorescence microscopy. Dynein (green) is shown in panels A, D, G and J, actin filaments (red) in the same samples in B, E, H and K, and overlaid images in C, F, I and L. (A-C) resting acini; (D-F) CCH-stimulated acini (100 μM, 15 minutes); (G-I) nocodazole-treated acini (33 μM, 60 minutes); (J-L) nocodazole-treated acini (33 μM, 60 minutes) exposed to CCH (100 μM, 15 minutes). Asterisk, lumenal regions; arrowhead, punctate labeling. Bar, ~10 μm.

Fig. 2 shows the distribution of p150^{Glued} and Arp1 in resting and CCH-stimulated acini. Like dynein, p150^{Glued} (Fig. 2A) and Arp1 (Fig. 2C) were detected in a diffuse pattern in resting acini. CCH stimulation promoted the same remarkable recruitment of p150^{Glued} (Fig. 2B) and Arp1 (Fig. 2D) into the subapical region detected for dynein. Analysis of the dynamitin distribution also revealed comparable diffuse and subapical (data not shown) accumulation patterns in resting and CCH-stimulated acini, respectively.

Our previous investigations defined conditions for nocodazole exposure that promoted disassembly of lacrimal acinar MTs (da Costa et al., 1998). Nocodazole comparably altered the resting distributions of dynein (Fig. 1G,I) and

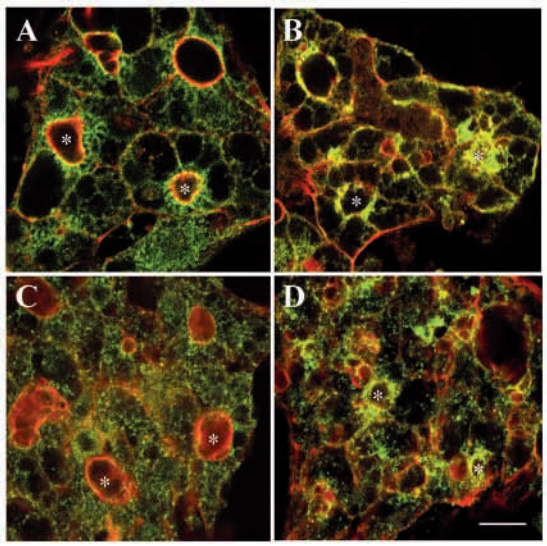

Fig. 2. CCH promotes recruitment of p150^{Glued} and Arp1 to the subapical region of acini. Lacrimal acini were fixed and processed for labeling of p150^{Glued} or Arp1 with actin filaments and imaged by confocal fluorescence microscopy. Panels A and B show p150^{Glued} (green) and actin filaments (red) in resting and CCH-stimulated (100 μM, 15 minutes) lacrimal acini, respectively, whereas panels C and D show Arp1 (green) and actin filaments (red) in resting and CCH-stimulated (100 μM, 15 minutes) lacrimal acini, respectively. Asterisk, lumenal regions. Bar, ~10 μm.

p150^{Glued} (data not shown), increasing punctate labeling (arrowhead) while decreasing diffuse labeling. Nocodazole also reduced CCH-induced accumulation of dynein (Fig. 1J,L) and p150^{Glued} (data not shown) beneath the apical membrane.

CCH significantly increases dynactin recovery in a protein fraction enriched in cytoskeletal and membrane proteins

To determine whether the CCH-induced subapical accumulations of dynein and the dynactin complex were associated with changes in their association with subcellular fractions, we subjected resting and CCH-stimulated acini to sequential detergent extraction into buffers containing saponin, Tx-100 and SDS. Analysis of the abundance (actin, tubulin, polymeric immunoglobulin A receptor or pIgAR, VAMP2, rab3D) or activity [lactate dehydrogenase (LDH)] of several proteins was used to define the composition of each pool (Table 1). The pool distributions of these proteins were not markedly affected by CCH. The presence of most of the actin and tubulin in the Tx-100 insoluble, SDS soluble pool was consistent with the enrichment of cytoskeletal filaments in this pool. Most cellular pIgAR (~65%), rab3D (~75%) and considerable stores of VAMP2 (~45%) were recovered in Tx-100 soluble pools, consistent with enrichment of membrane proteins in this pool. However, ~20% of total pIgAR and rab3D as well as ~35% of total VAMP2 were recovered in Tx-100 insoluble, SDS soluble fractions, representing proteins associated with Tx-100 insoluble membranes or cytoskeleton. Approximately 15-20% of pIgAR and VAMP2 stores were recovered in saponin soluble pools, possibly reflecting release of some membranes with saponin. Lacrimal acinar LDH has previously been identified in cytosol and within secretory membranes (Thurig et al., 1984). Consistent with this, most LDH activity (~70%) was recovered in saponin soluble fractions with approximately 25% recovered in Tx-100 soluble fractions. We conclude that the proteins recovered in saponin soluble fractions are primarily cytosolic proteins, those recovered in Tx-100 soluble fractions are primarily membrane proteins, and those recovered in SDS soluble fractions include a mixture of cytoskeletal and Tx-100 insoluble membrane proteins.

Fig. 3 shows that approximately 60% of total p150^{Glued} and Arp1 are recovered in the Tx-100 insoluble, SDS soluble pool from resting acini, with the remainder split between saponin soluble and Tx-100 soluble pools. CCH stimulation elicited a small but significant ($P \leq 0.05$) increase in the recovery of both dynactin components with the Tx-100 insoluble, SDS soluble pool, with a concomitant depletion in their stores from the other two pools. DIC distribution across these pools was assessed; approximately 40% of cellular DIC was recovered in the Tx-100 insoluble, SDS soluble pool from resting acini, with the remainder distributed equally between the other two pools. No significant change in DIC association across pools was caused by CCH treatment. These findings suggest that CCH promotes redistribution of dynactin to a Tx-100 insoluble, SDS soluble pool enriched in cytoskeleton and membrane proteins.

CCH increases the colocalization of VAMP2 with dynein and dynactin in the subapical region

The CCH-sensitive recruitment of dynein and dynactin into the subapical region under conditions associated with apical exocytosis suggested that dynein might facilitate movement of secretory membranes. The distribution of two effectors of the secretory pathway, rab3D and VAMP2, were investigated in parallel with dynein and the dynactin complex. Rab3D

Table 1. Recovery of marker proteins in pools isolated by sequential detergent extraction in resting and CCH-stimulated lacrimal acini

	Resting lacrimal acini			Stimulated lacrimal acini		
Marker proteins	Saponin (% of total)	Tx-100 (% of total)	SDS (% of total)	Saponin (% of total)	Tx-100 (% of total)	SDS (% of total)
Actin	25.0±1.4	23.0±2.5	52.0±3.7	22.0±1.4	21.4±1.7	56.5±1.3
LDH	67.4±2.4	26.1±2.3	6.5±1.8	71.9±2.9	22.6±2.5	5.6±1.5
Tubulin	8.9±1.6	8.1±0.5	83.0±1.2	8.7±1.1	8.9±3.1	82.5±2.6
pIgAR	15.0±3.0	62.9±3.9	22.1±3.2	17.7±3.4	64.9±0.9	17.4±4.3
VAMP2	19.1±4.8	49.7±9.0	31.3±7.3	18.4±5.6	43.8±7.9	37.8±5.6
Rab3D	5.8±2.2	81.1±3.4	13.0±1.7	9.3±2.6	69.6±4.9	21.1±5.4

Values represent the mean ± s.e.m. from 3-10 experiments. Stimulation used 100 μM CCH for 15 minutes.

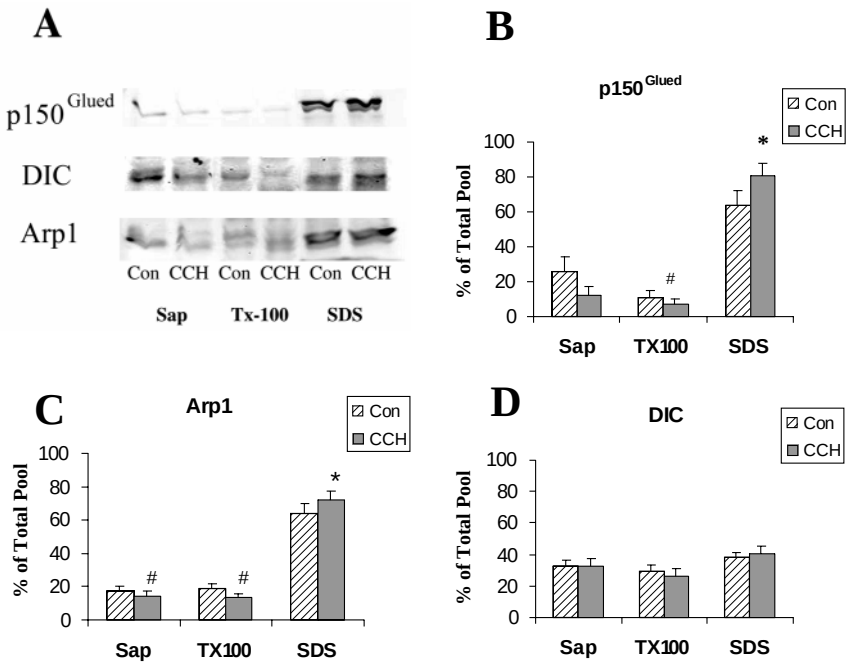

Fig. 3. CCH increases recovery of p150^{Glued} and Arp1 in Triton X-100 insoluble, SDS soluble fractions. Lacrimal acini were treated without (Con) or with CCH (100 μM, 15 minutes) before sequential extraction into buffers containing saponin (Sap), Tx-100 and SDS. (A) Western blots of detergent eluates from representative preparations of Con and CCH-treated lacrimal acini showing p150^{Glued}, Arp1 and DIC contents in each pool. Blots used appropriate primary and IRDye™800-conjugated secondary antibodies. Equal volumes of each pool were loaded, with protein assays confirming that CON and CCH detergent eluates within each pool had equivalent protein contents. (B-D) Summary of changes in p150^{Glued}, Arp1 and DIC recovery in each eluate from Con and CCH-stimulated acini expressed as a percentage of the total cellular content of each protein. *n*=7-10 preparations; error bars represent s.e.m.; *Significant increase at $P<0.05$; #significant decrease at $P<0.05$.

immunoreactivity was concentrated primarily in the subapical region in resting acini (Fig. 4K). This large subapical pool was rapidly depleted by CCH stimulation, resulting in dispersal of rab3D labeling throughout the cell with retention of traces of residual rab3D beneath the apical membrane (Fig. 4K'). VAMP2 immunoreactivity was dispersed throughout the cytoplasm of resting acini, with traces associated with the apical membrane (Fig. 4B,E,H). CCH stimulation increased VAMP2 immunoreactivity in the subapical region and at the apical plasma membrane (Fig. 4B',E',H'). The changes in these proteins in response to CCH suggested that rab3D-enriched membranes represent mature secretory vesicles located beneath apical membrane; release of their stores constitutes the initial response to secretagogue. VAMP2-enriched membranes may represent a recruitable vesicle population transported into the subapical region to sustain the secretory response.

Dual labeling of VAMP2 with dynein and dynactin complex constituents in resting acini revealed traces of colocalization of DIC, Arp1 and p150^{Glued} (arrows, Fig. 4C,F,I). However, CCH stimulation resulted in substantial increases in colocalization of DIC (Fig. 4C'), Arp1 (Fig. 4F') and p150^{Glued} (Fig. 4I') with the VAMP2 stores specifically in the subapical region (arrows). Dual labeling experiments with p150^{Glued} or DIC (data not shown) and rab3D revealed traces of colocalization in the subapical region of resting acini (Fig. 4L, arrowheads), which were not increased by CCH (Fig. 4L').

Increased recovery of dynein and VAMP2 in membranes isolated by MT-affinity from CCH-treated acini

To obtain additional evidence in support of dynein-driven transport of VAMP2-enriched membranes into the subapical region, we used MT-affinity membrane isolation. This technique isolates membranes containing active motors based on their ability to cosediment with taxol-stabilized MTs and to be released in the presence of excess Mg-ATP. As shown in Fig. 5, western blotting of equivalent amounts of protein obtained from microsomal membranes isolated by MT-affinity, ATP release revealed a significant ($P\leq0.05$) increase in the recovery of dynein and VAMP2 in membranes from CCH-stimulated acini relative to resting acini. Rab3D was undetectable by western blotting of these samples (data not shown).

Association of dynein and dynactin with isolated membrane compartments

Previous studies have used sorbitol density gradient centrifugation to isolate subcellular membranes and to map the trafficking between them (Gierow et al., 1996; Hamm-Alvarez et al., 1997; Yang et al., 1999; Qian et al., 2002). We therefore applied this technique to membranes from resting and CCH-stimulated acini to further understand the contributions of dynein to apically targeted secretory traffic.

p150^{Glued} and Arp1 immunoreactivities (Fig. 6A) associated with membranes from resting acini exhibited similar distributions, with major concentrations in fractions 7-10. DIC was present in the same fractions (Fig. 6A), but it was relatively more abundant in fractions 11, 12 and P than dynactin. β-Hexosaminidase (Fig. 6A), which is both a lysosomal and a secretory protein in lacrimal acini, resembled p150^{Glued} and Arp1 but compared to these markers, it was slightly more abundant in fractions 11-P. Total membrane protein (Fig. 6A) resembled β-hexosaminidase.

In resting acini, rab3D exhibited a pronounced concentration in fraction 1 (Fig. 6B), probably reflecting the presence of fragments derived from a specialized microdomain of mature secretory vesicle membranes. In addition, rab3D was broadly distributed across the gradient. The major component resembled p150^{Glued} and Arp1, but, compared to p150^{Glued} and Arp1, rab3D was relatively more abundant in fractions 4-6. Acid phosphatase (Fig. 6B) was broadly distributed, but, somewhat like rab3D, it was also abundant in fraction 1. The

resting distributions of VAMP2 and γ-adaptin (Fig. 6B) resembled that of rab3D in the higher density regions of the gradient. Unlike rab3D, they were not particularly abundant in fraction 1, but, like rab3D, they were relatively more abundant than p150^{Glued} and Arp1 in fractions 5-6. Consistent with its primary localization in the trans-Golgi network (TGN), a complex structure organized into multiple functionally distinct microdomains, rab6 appeared associated with three compartments, centered in fractions 4-5, 7-8 and 10-12 (Fig. 6B).

CCH stimulation promoted the following parallel changes in DIC, p150^{Glued} and Arp1: relative depletions centered at fraction 8 and concomitant increases in fraction 5 and fraction P. These changes were statistically significant ($P \leq 0.05$) for at least one of the three proteins, with the same trend reflected for the others (see change plots in Fig. 6A). CCH stimulation was also associated with several additional apparent redistributions: β-hexosaminidase from fractions 7-8 to P, protein from 7-10 to P, rab6 from 7-10 to 2-3, rab3D from 1 to 4-5, and acid phosphatase from 1 to 4-6. CCH stimulation had no significant effects on VAMP2 and γ-adaptin, but the data suggest possible redistributions of these markers to pooled fractions 11-P.

These findings as well as our data from previous studies probing the identity of membrane compartments in acini using this method (Gierow et al., 1996; Hamm-Alvarez et al., 1997; Yang et al., 1999; Qian et al., 2002) suggested that in resting acini dynein, dynactin and VAMP2 are associated with biosynthetic and sorting compartments, and that dynein is additionally associated with pre-lysosomal and lysosomal compartments. The CCH-associated redistributions of dynein and dynactin complex, as well as β-hexosaminidase, suggest movement away from biosynthetic compartments to higher density compartments. In contrast, the redistributions of rab3D and acid phosphatase suggest movement from mature secretory vesicles to biosynthetic compartments. The redistribution of rab6 suggests pronounced changes or translocations within the TGN.

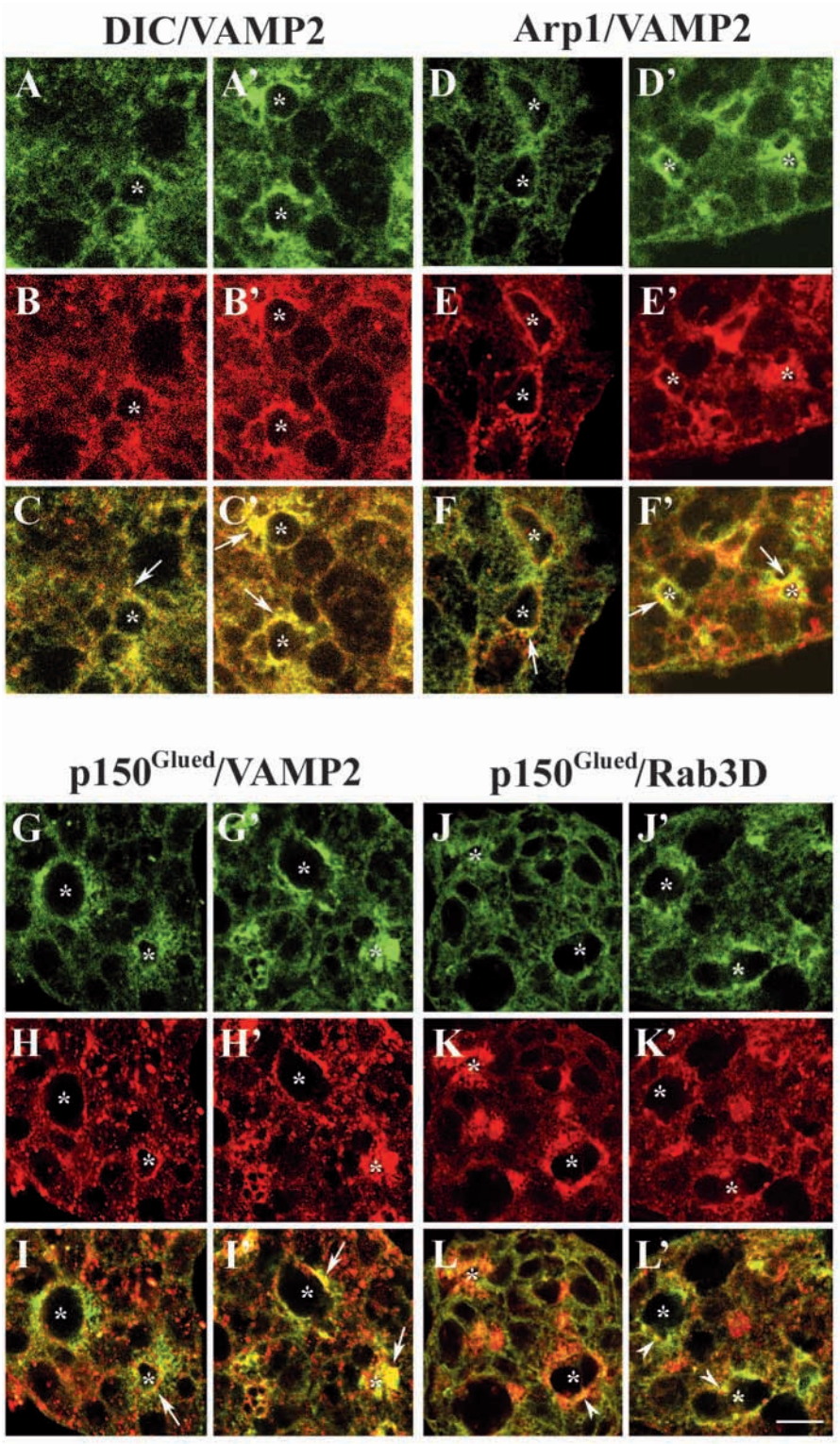

Fig. 4. CCH increases dynein and dynactin colocalization with VAMP2 in the subapical region of acini. Lacrimal acini were fixed and processed to label DIC, p150^{Glued} or Arp1 with rab3D or VAMP2 and imaged by confocal fluorescence microscopy. (A-L) Resting acini, whereas A'-L' depict CCH-stimulated (100 μM, 15 minutes) acini. A-C and A'-C' show DIC (green) and VAMP2 (red) separately (A,A',B,B') and overlaid (C,C'); D-F and D'-F' show Arp1 (green) and VAMP2 (red) separately (D,D',E,E') and overlaid (F,F'); G-I and G'-I' show p150^{Glued} (green) and VAMP2 (red) separately (G,G',H,H') and overlaid (I,I'); and J-L and J'-L' show p150^{Glued} (green) and rab3D (red) separately (J,J',K,K') and overlaid (L,L'). Arrows and arrowheads, regions of colocalization of dynein or dynactin with VAMP2 or rab3D, respectively. Asterisk, lumenal regions. Bar, ~10 μm.

Given the extensive overlap of these compartments on the sorbitol density gradients, we introduced a second separation dimension by conducting phase partitioning in an aqueous, dextran-polyethyleneglycol two-phase system. Phase partitioning is a liquid chromatography procedure that separates membranes according to their distribution between stationary (dextran-rich) and mobile (polyethyleneglycol-rich) phases. Fraction numbering begins at the origin that contains membranes preferring the stationary phase.

Fig. 7 depicts the distributions of DIC, p150^{Glued} and other markers among the isolated compartments after phase partitioning analysis of density gradient fractions from CCH-stimulated acini. Partitioning of fractions 11-P revealed comigration of VAMP2, p150^{Glued} and β-hexosaminidase with a dynein-rich compartment (peak j in Fig. 7). Similarly, partitioning of fraction P revealed comigration of dynein, p150^{Glued} VAMP2 and traces of β-hexosaminidase in another population (peak m in Fig. 7). We propose that these membrane populations contain VAMP2-enriched secretory transport vesicles driven into the subapical region by dynein. In addition, considerable amounts of dynein, the dynactin complex and VAMP2 are associated with a series of Golgi- and TGN-related compartments that contain varying amounts of rab6, γ-adaptin and rab3D (labeled b, c, d, f, g, h and i in Fig. 7).

Overexpression of dynamitin in lacrimal acini using replication-deficient Ad

Dynamitin overexpression offered the possibility to directly test whether (1) dynein activity was required for movement of VAMP2-enriched membranes into the subapical region and (2) dynein activity was important in basal and/or CCH-stimulated secretion. Conditions of exposure to replication-incompetent Ad vectors were identified that resulted in reproducible, high-efficiency (70-90%) transduction of lacrimal acini with β-galactosidase (Fig. 8A,B) or GFP (Fig. 8C,D). Likewise, untransduced acini exhibited a diffuse cytoplasmic dynamitin labeling pattern because of endogenous protein (Fig. 8E), whereas acini transduced with Ad-Dynt and imaged at comparable settings exhibited an intense cytoplasmic fluorescence in almost all cells (Fig. 8F). Dynamitin overexpression relative to levels in untransduced acini was confirmed by ^{35}S-labeling of cellular proteins and analysis by SDS-PAGE and autoradiography (Fig. 8G), and by western blotting of extracts from Ad-Dynt- and Ad-Dynt-GFP-transduced acini (Fig. 8H). Dynamitin overexpression in acini transduced with Ad-Dynt and Ad-Dynt-GFP was 395±70% and 363±63% of untransduced acini, respectively (n=7).

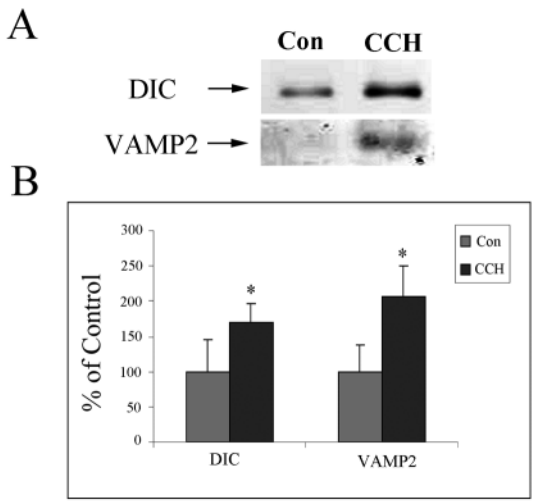

Fig. 5. MT-affinity isolation of subcellular membranes from resting and CCH-stimulated acini. Lacrimal acini were incubated without (Con) and with CCH (100 μM, 15 minutes) and processed to isolate membranes using MT-affinity and release with excess ATP. Western blots using appropriate primary and IRDye™800-conjugated secondary antibodies from a representative preparation are shown in A, whereas B depicts summary data showing the contents of DIC and VAMP2 in MT-affinity, ATP release fractions under each condition. 40 μg of protein from resting and CCH-stimulated membrane samples were loaded under each condition. n=4-5 separate preparations. *Significant increase at P≤0.05.

Dynamitin overexpression inhibits CCH-stimulated recruitment of p150^{Glued}, DIC and VAMP2 to the subapical region

Resting acini transduced with Ad-LacZ exhibited diffuse labeling patterns for p150^{Glued} and DIC (Fig. 9A,B, respectively), whereas CCH stimulation of these acini promoted the accumulation of p150^{Glued} and DIC into the subapical region characteristic of untreated acini (Fig. 9A',B', respectively). Similarly, Ad-LacZ transduction did not affect either the CCH-dependent recruitment of VAMP2 into the subapical region nor its colocalization (arrows) with p150^{Glued} (compare Fig. 9E and Fig. 9E') or DIC (compare Fig. 9F and Fig. 9F'). P150^{Glued} and DIC in Ad-Dynt transduced resting acini exhibited a punctate labeling pattern (arrowheads, Fig. 9C,D, similar to nocodazole-treated acini, see also Fig. 2). CCH stimulation of Ad-Dynt-transduced acini exhibited no accumulation of p150^{Glued} or DIC in the subapical region (Fig. 9C',D', respectively). Ad-Dynt also prevented the CCH-

Table 2. Comparison of the enrichment of Arp1 in pools isolated by sequential detergent extraction in resting and CCH-stimulated lacrimal acini exposed to Ad constructs

	Resting lacrimal acini			Stimulated lacrimal acini		
Treatment	Saponin (% of total)	Tx-100 (% of total)	SDS (% of total)	Saponin (% of total)	Tx-100 (% of total)	SDS (% of total)
Untreated	17.5±5.7	16.2±5.0	66.3±10.4	16.4±6.2	12.4±3.8†	**71.2±9.8***
Ad-LacZ	21.0±6.4	19.9±2.8	59.1±9.1	21.4±7.3	14.6±2.6†	**64.0±9.3***
Ad-Dynt	20.4±2.3	19.8±1.7	59.7±3.8	19.3±3.4	17.1±3.1	**63.6±4.6***

Values represent the mean ± s.e.m. from 4-5 experiments. Stimulation used 100 μM CCH for 15 minutes.
*Significant increase from unstimulated acini under the same treatment conditions at P≤0.05 (highlighted in bold).
†Significant decrease from unstimulated acini under the same treatment conditions at P≤0.05.

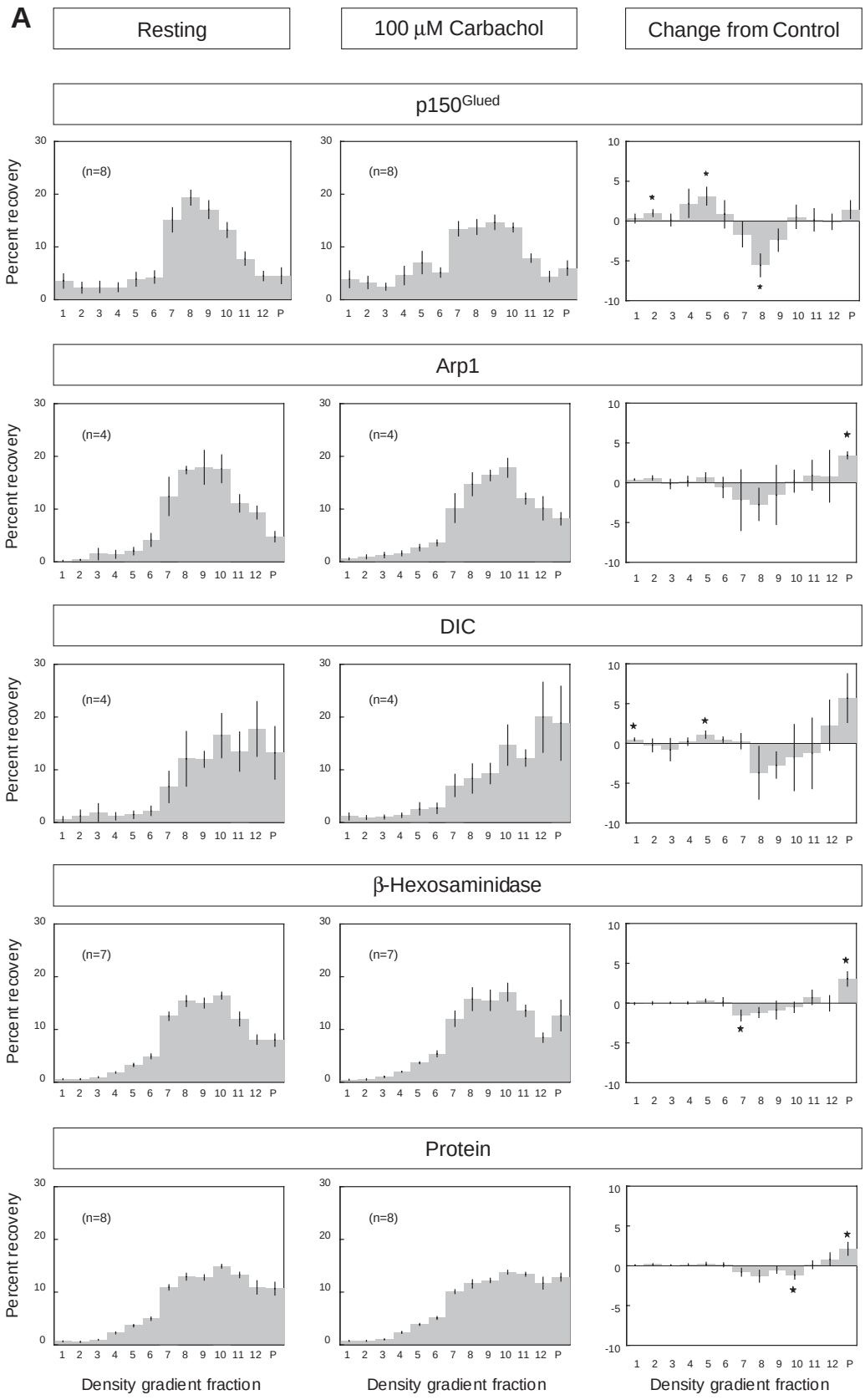

Fig. 6. Dynein, dynactin and secretory and biosynthetic compartment markers after density gradient analysis of resting and CCH-stimulated acini. Lacrimal acini incubated without (resting) and with CCH (100 μM, 15 minutes) were processed by isopycnic centrifugation on sorbitol density gradients. (A) The distributions of p150^{Glued}, Arp1, DIC, β-hexosaminidase and total protein. (B) The distributions of VAMP2, γ-

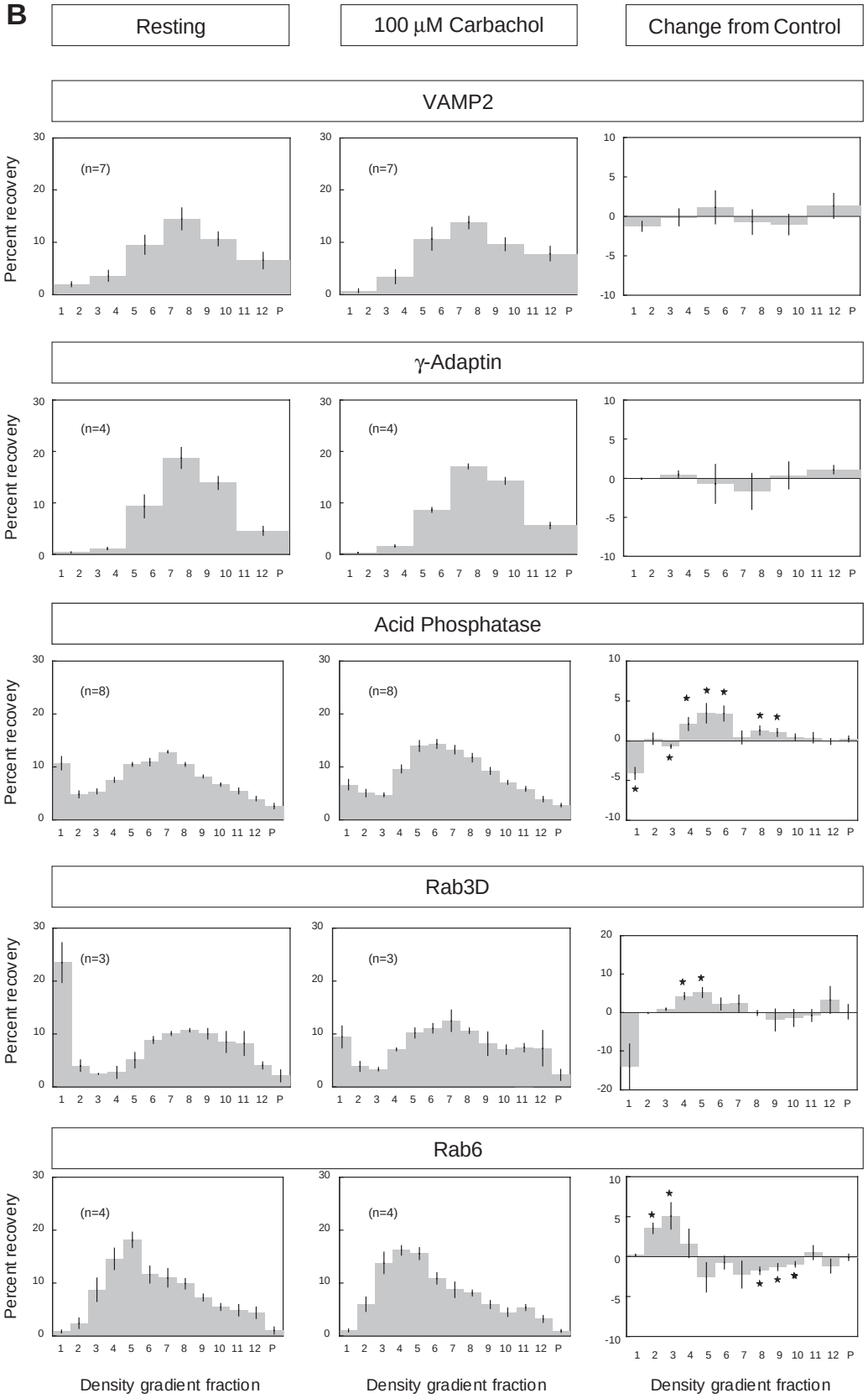

adaptin, acid phosphatase, rab3D and rab6. Fractions were pooled for VAMP2 and γ-adaptin to conserve material for western blotting. Left and middle columns show distributions of markers from resting and CCH-stimulated acini, respectively, whereas the right columns show CCH-induced changes. *n*=3-8 preparations; error bars represent s.e.m. **P*<0.05.

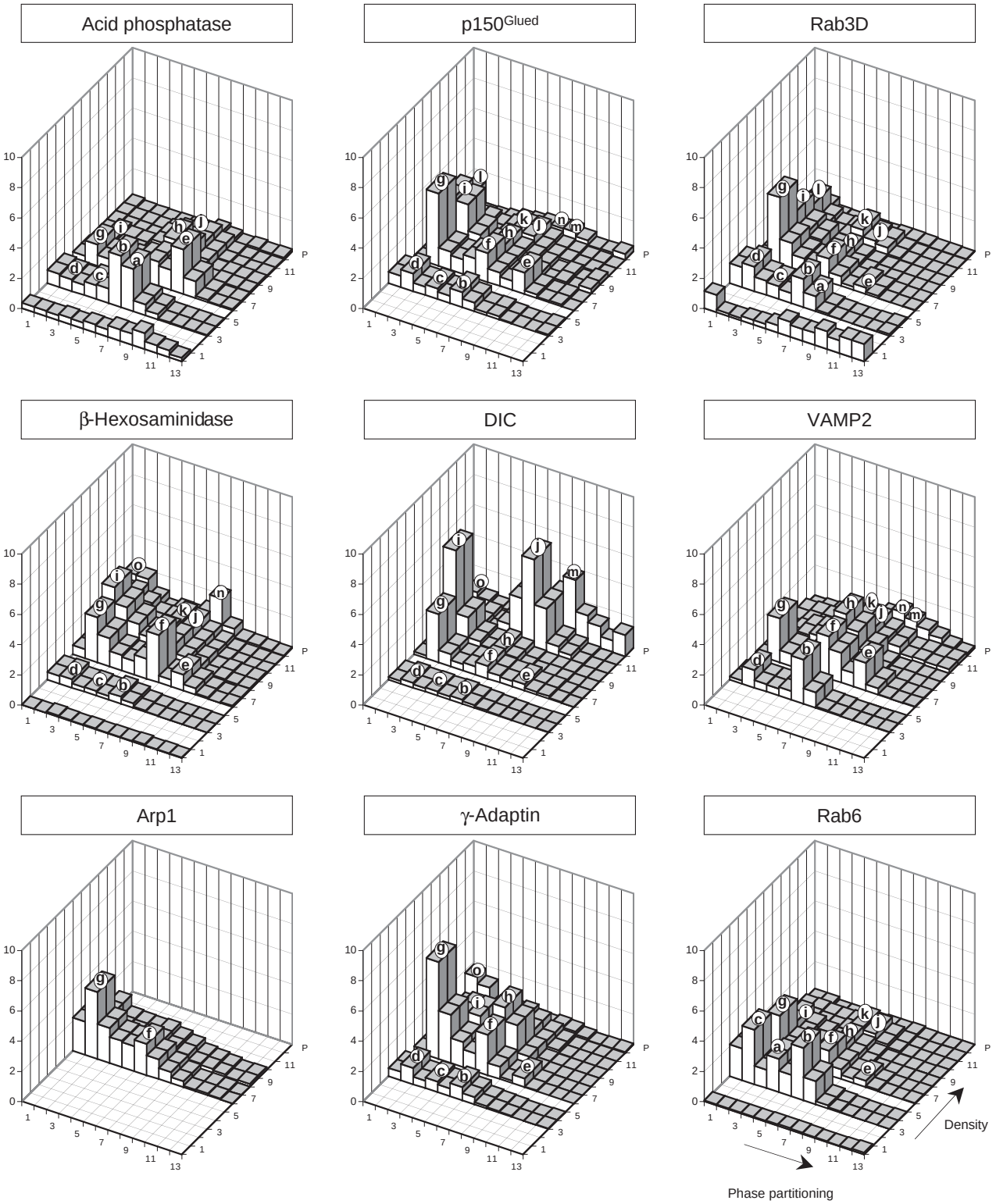

Fig. 7. Dynein, dynactin and membrane compartment markers after phase partitioning analysis of density gradient fractions. Density gradient fractions from CCH-stimulated acini were analyzed by partitioning in an aqueous dextran-polyethyleneglycol two-phase system. Gradient fractions 1 and P were analyzed individually; other fractions were pooled as follows: 4+5, 7+8, 9+10, 11+12. Modal positions of compartments are designated by a-o. Compartments j and m are proposed to contain secretory transport vesicles and related compartments [recruitable secretory vesicles (rsv) and immature secretory vesicles (isv)]. Other compartment designations are discussed in detail by Qian et al. (Qian et al., 2002). (a) Basal-lateral recycling endosome; (e) Basal-lateral sorting endosome; (b-d,f,h,i) Specialized TGN microdomains; (g) Golgi complex; (k) Secretory vesicle membrane fragments; (l,o) Pre-lysosomes; (n) Lysosomes. Similar results were obtained in a second analysis with a different phase system composition.

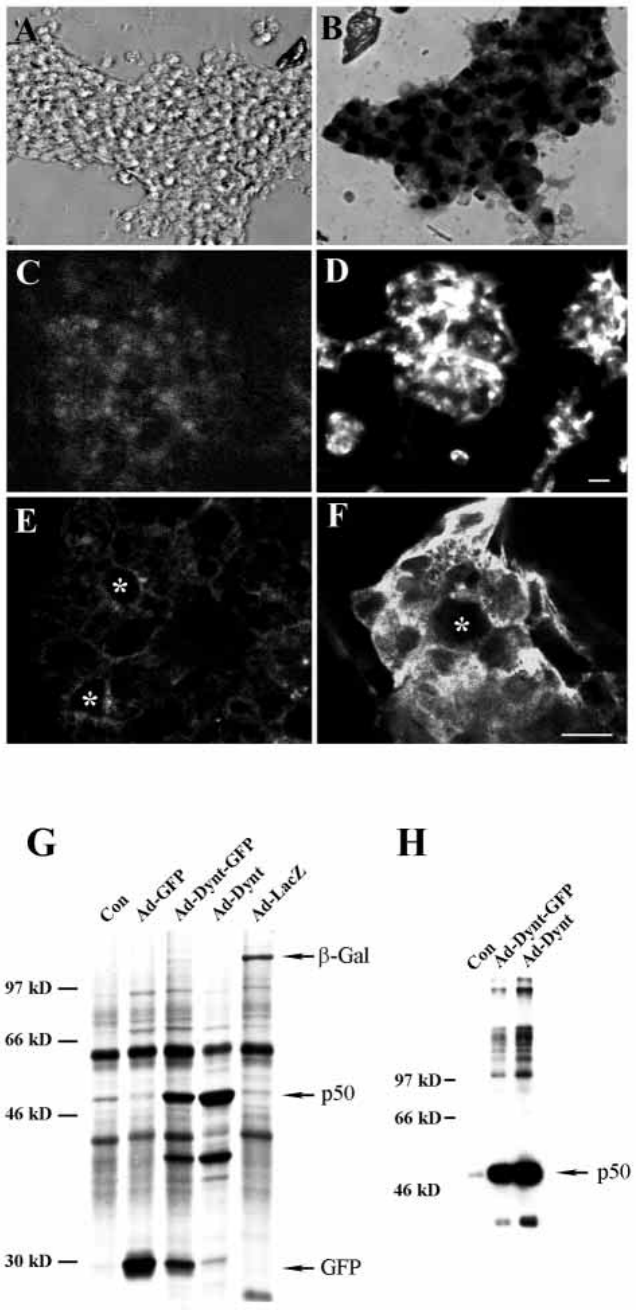

Fig. 8. Transduction of acini with Ad constructs. (A,B) Phase microscopy images of untransduced and Ad-LacZ-transduced acini, respectively, processed for detection of β-galactosidase activity with X-Gal as substrate. (C,D) Fluorescence microscopy images of untransduced and Ad-GFP-transduced acini, respectively. (E,F) Confocal fluorescence microscopy images of untransduced and Ad-Dynt-transduced acini, respectively, processed for detection of dynamitin by immunofluorescence. (G) The spectrum of ^{35}S-labeled proteins obtained by autoradiography of proteins from control and transduced acini resolved by SDS-PAGE. Arrows indicate positions of β-galactosidase (β-Gal), GFP and dynamitin (p50). H shows dynamitin content in lysates from untransduced (Con), Ad-Dynt-transduced and Ad-Dynt-GFP transduced acini by western blotting. Transduction with constructs was at a MOI of 5 PFU/cell for 4 hours followed by rinsing and recovery for 16-18 hours. Bars in D and F represent 10 μm and reflect magnifications in A-D and E-F, respectively. Asterisk, lumenal regions.

dependent enrichment of VAMP2 and its colocalization with p150^{Glued} (compare Fig. 9G and 9G') and DIC (compare Fig. 9H and 9H').

To confirm that dynamitin overexpression was specifically inhibiting dynein-based movement of membranes in CCH-stimulated acini, we investigated whether CCH-induced Arp1 recruitment to membranes was affected. Dynamitin overexpression is thought to prevent the interaction of the two structural motifs of dynactin, the Arp1 filament and the p150^{Glued} sidearm; therefore, its overexpression should not alter CCH-stimulated recruitment of Arp1 to membranes. Fig. 10A and 10A' show the localization of Arp1 in Ad-LacZ-transduced resting and CCH-stimulated acini, respectively. As seen in these images and the overlaid images in Fig. 10E and Fig. 10E', Arp1 is clearly recruited into the subapical region following CCH stimulation where it is colocalized with VAMP2, comparable to the response in untransduced acini (Fig. 4). Fig. 10B and Fig. 10B' show the localization of Arp1 in Ad-Dynt-transduced resting and CCH-stimulated acini, respectively. CCH stimulation of Ad-Dynt-transduced acini is associated with increased punctate Arp1 fluorescence distributed throughout the cytoplasm relative to untransduced acini, suggesting increased association with subcellular membranes. Fig. 10F' also shows that there is increased colocalization of Arp1 and VAMP2 (arrowheads) throughout the cytoplasm of CCH-stimulated Ad-Dynt-transduced acini, although these components are not recruited into the subapical region.

We analyzed the effects of dynamitin overexpression on CCH-stimulated recruitment of Arp1 to the Tx-100 insoluble, SDS soluble pool using sequential detergent extraction. Table 2 shows the enrichment of Arp1 in saponin soluble, Tx-100 soluble and SDS soluble pools from resting and CCH-stimulated untransduced acini and acini transduced with Ad-LacZ or Ad-Dynt. The effects under all conditions were comparable, revealing a small but statistically significant ($P \leq 0.05$) increase in Arp1 recovery with Tx-100 insoluble, SDS soluble fractions comparable in magnitude to that shown previously (Fig. 3). Moreover, the percentage recovery of Arp1 within each pool in resting and CCH-stimulated acini under each condition was not significantly different.

Dynamitin overexpression and nocodazole treatment deplete rab3D beneath the apical membrane

Although only traces of overlap between p150^{Glued} and rab3D were detected by confocal fluorescence microscopy (Fig. 4), a contribution of dynein and MTs to maintenance of this vesicle population was suggested by the finding that nocodazole treatment abolished subapical stores of rab3D in unstimulated acini (compare Fig. 11E and Fig. 11F). We examined the effects of dynamitin overexpression on rab3D-enriched membrane vesicles. Transduction with Ad-Dynt markedly reduced subapical stores of rab3D in resting acini relative to untransduced acini (compare Fig. 11C versus Fig. 11A). However, some dispersal of the subapical pool of rab3D was also elicited by Ad-LacZ (Fig. 11B) and Ad-GFP (data not shown) in resting acini. In order to distinguish between the non-specific effects of Ad vector and the specific effects of dynamitin overexpression, we quantified the rab3D labeling pattern in untransduced (control) and transduced acini. The labeling

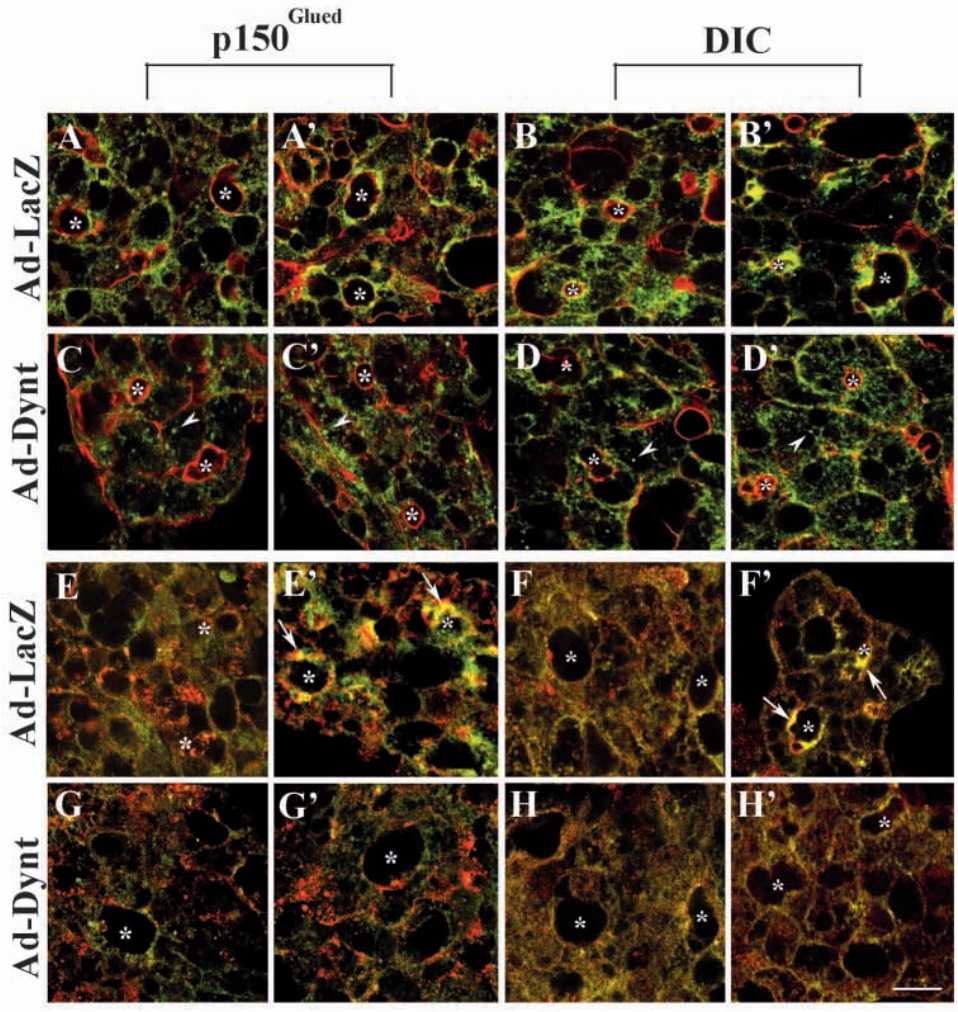

Fig. 9. Dynamitin overexpression inhibits CCH-stimulated recruitment of DIC, p150^{Glued} and VAMP2 to the subapical region. Resting and CCH-stimulated (100 μM, 15 minutes) lacrimal acini transduced with Ad-LacZ or Ad-Dynt were fixed and processed for detection of p150^{Glued} (green, A-A',C-C',E-E',G-G') or DIC (green, B-B',D-D',F-F',H-H') with actin filaments (red, A-D,A'-D') or VAMP2 (red, E-H,E'-H') and imaged by confocal fluorescence microscopy. (A-H,A'-H') Resting and CCH-stimulated (100 μM, 15 minutes) acini, respectively. A-A', B-B', E-E' and F-F' were transduced with Ad-LacZ and C-C', D-D', G-G' and H-H' were transduced with Ad-Dynt. Arrowheads, punctate labeling; arrows, colocalization of DIC or p150^{Glued} with VAMP2; asterisk, lumenal regions. Bar, 10 μm.

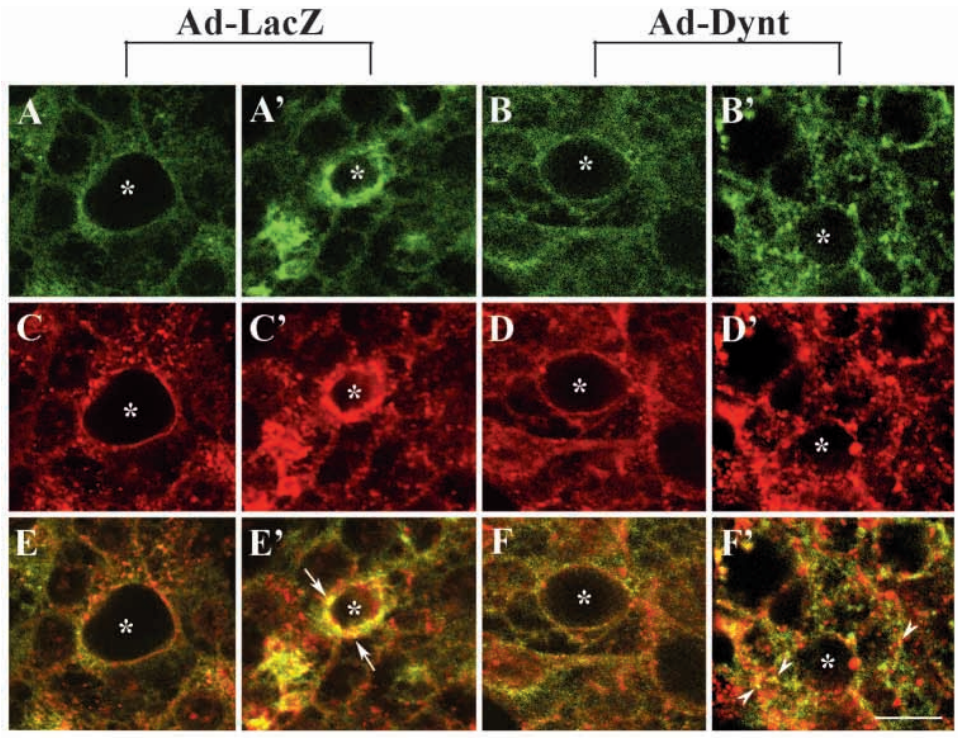

Fig. 10. Dynamitin overexpression promotes increased cytoplasmic colocalization of VAMP2 and Arp1 in CCH-stimulated acini. Resting and CCH-stimulated lacrimal acini transduced with Ad-LacZ or Ad-Dynt were fixed and processed for detection of Arp1 (A-A' and B-B') and VAMP2 (C-C' and D-D'). (E-E' and F'F') Colocalization of these markers. (A-A', C-C' and E'E') Acini transduced with Ad-LacZ; (B-B', D-D' and F-F') Acini transduced with Ad-Dynt. (A-F) Resting acini; (A'-F') CCH-stimulated (100 μM, 15 minutes) acini. Bar, 10 μm. (*) Lumenal regions; arrowheads, colocalization of Arp1 and VAMP2 in the cytoplasm; arrows, colocalization of Arp1 and VAMP2 beneath the apical membrane.

pattern was categorized into one of three classes: dispersed, half apical (concentrated in the apical half of the cell) and mostly apical. As shown in Fig. 11D, only ~19% of the lumenal regions in control acini showed dispersed rab3D labeling, with ~44% of lumenal regions exhibiting compact apical labeling and ~37% exhibiting half apical labeling. In contrast, ~78% of the lumenal regions in Ad-Dynt-transduced acini showed dispersed rab3D labeling, with ~19% showing half apical labeling and only ~3% showing apical labeling. Rab3D distribution in Ad-LacZ-transduced acini was intermediate between these values, exhibiting ~45% of labeling in a dispersed pattern and retaining ~39% as half apical and ~17% as apical. As shown in Fig. 11G and Fig. 11H, respectively, transduction with Ad-LacZ or Ad-Dynt did not alter the organization or abundance of apical MTs. Although the non-specific effects elicited by Ad-LacZ necessitate interpretation of these data with some caution, the comparable effects elicited by nocodazole suggest that dynein-driven vesicle transport may be important for maintenance of rab3D-enriched vesicles.

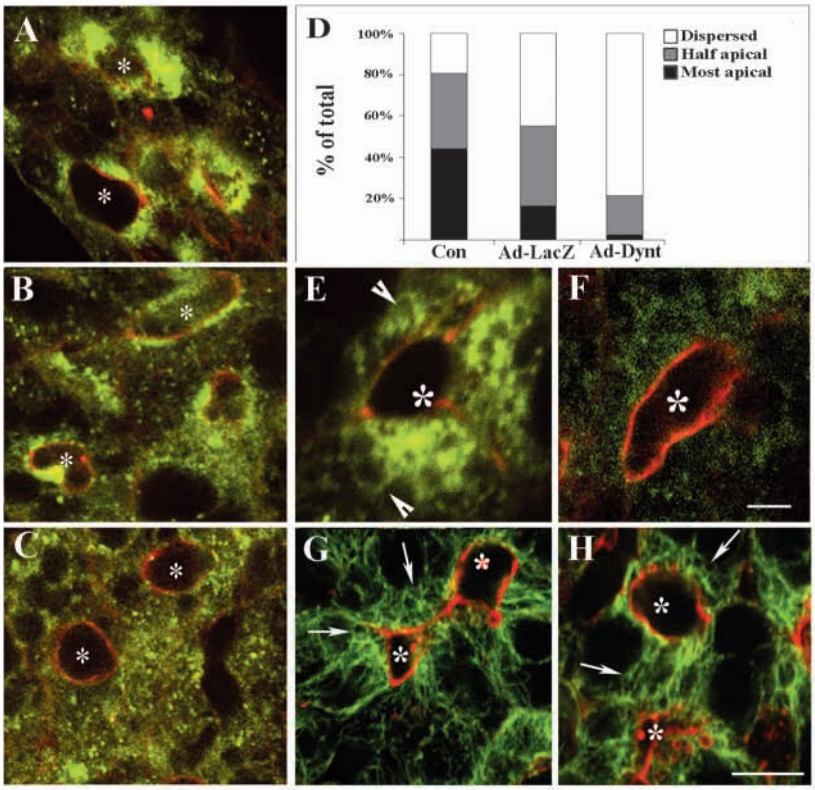

Fig. 11. Dynamitin overexpression or nocodazole treatment reduce the subapical accumulation of rab3D in resting acini. Untransduced (Con) and transduced rabbit lacrimal acini were fixed and processed for detection of rab3D (green, A-C,E,F) or MTs (green, G and H) in parallel with actin filaments (red). (A,B,C) rab3D and actin filaments in untransduced, Ad-LacZ-transduced and Ad-Dynt-transduced acini, respectively. (D) rab3D distribution quantified into three categories from 366-404 lumena from 3-4 separate preparations under each condition: apical, half apical and fully dispersed. (E,F) rab3D labeling beneath actin-enriched lumenal regions in untreated and nocodazole-treated (33 μM, 60 minutes) acini, respectively. Arrowheads indicate rab3D-enriched secretory vesicles. (G,H) MTs and actin filaments in Ad-LacZ-transduced and Ad-Dynt-transduced acini, respectively. Arrows indicate MTs extending from the apical pole; asterisk, lumenal regions. Bar in F, 6 μm. Bar in H, 10 μm.

Dynamitin overexpression modifies CCH-independent and CCH-dependent secretion of protein and β-hexosaminidase

Basal, total and stimulated release of bulk protein and the secretory protein, β-hexosaminidase, were measured in lacrimal acini transduced with Ad-GFP or Ad-Dynt-GFP (Fig. 12). Total protein and β-hexosaminidase release in CCH-stimulated acini were not significantly altered by dynamitin overexpression. When we resolved the contributions of basal and CCH-stimulated release to total release, we found that Ad-Dynt-GFP elicited a significant ($P \leq 0.05$) increase in basal (CCH-independent) release of protein with a similar but not statistically significant trend noted for β-hexosaminidase. Dynamitin overexpression also caused a significant ($P \leq 0.05$) decrease in the component of total protein and β-hexosaminidase release triggered by CCH, by 58% and 69%, respectively. These changes in the proportion of total secretory products released in a CCH-independent versus CCH-dependent manner were not directly attributable to decreased protein synthesis, because labeling experiments using ^{35}S-Translabel revealed that bulk protein synthesis in acini transduced with Ad-GFP or Ad-Dynt-GFP was actually slightly elevated relative to bulk protein synthesis in untransduced acini (data not shown). We suggest that dynein inhibition impairs the ability of acini to sequester secretory proteins in the regulatable arm of the secretory pathway, allowing their release through a constitutive pathway. This effect may be related

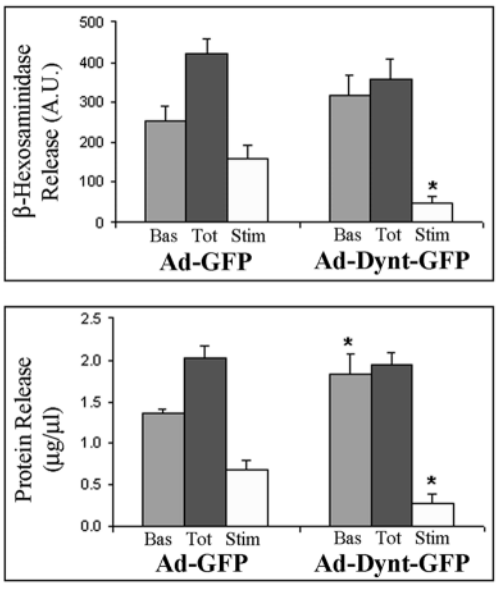

Fig. 12. Dynamitin overexpression modifies CCH-independent and CCH-dependent release of bulk protein and β-hexosaminidase. Lacrimal acini cultured on Matrigel-coated 24-well plates were transduced with Ad-GFP or Ad-Dynt-GFP, treated without or with CCH (100 μM, 30 minutes) and processed for measurement of basal (Bas), total (Tot) and stimulated (Stim) protein and β-hexosaminidase release as described. n=6 preparations; *$P \leq 0.05$; A.U., arbitrary fluorescence unit.

to the depletion of rab3D-enriched mature secretory vesicles in Ad-Dynt-transduced acini (Fig. 11).

Discussion

This study investigates the participation of dynein-driven vesicle transport in stimulated secretory traffic to the apical membrane in lacrimal acini. Confocal fluorescence microscopy revealed a major CCH-induced, MT-dependent recruitment of cytoplasmic dynein and the dynactin complex into the subapical region that was sensitive to nocodazole treatment (Figs 1 and 2) and inhibited by dynamitin overexpression (Fig. 9), suggesting that dynein activity drives this recruitment. This subapical enrichment of dynein and the dynactin complex was colocalized with VAMP2 (Fig. 4), suggesting that many of the vesicles transported by dynein towards the apical membrane were enriched in this protein. This hypothesized involvement of dynein in CCH-stimulated recruitment of VAMP2-enriched membranes towards the apical membrane is further supported by the following observations in CCH-stimulated acini: (1) the significant increase in dynein and VAMP2 abundance in MT-affinity-purified membranes from CCH-stimulated acini (Fig. 5); (2) the isolation of two high-density membrane populations enriched in dynein, VAMP2, β-hexosaminidase and dynactin by phase partitioning of density gradient fractions 11-P (peaks j and m, Fig. 7); and (3) the inhibition of transport of VAMP2-enriched membranes into the subapical region by dynamitin overexpression (Fig. 9). This model is also consistent with the increased recovery of Arp1 and $p150^{Glued}$ with Tx-100 insoluble, SDS soluble fractions already enriched in VAMP2 and DIC shown in Fig. 3 and Table 1. Although VAMP2-enriched membranes appear to constitute a substantial proportion of dynein's cargo, confocal fluorescence microscopy and biochemical analysis show that some VAMP2 and dynein are associated with other compartments. Some of the observed subapical accumulation of dynein and the dynactin complex in CCH-stimulated acini may also reflect stores associated with VAMP2-free membranes involved in the secretory response, for instance transcytotic vesicles or other TGN-derived vesicles.

Dynein activity may also be important for maintenance of the mature rab3D-enriched secretory vesicles already present in the subapical region which are rapidly discharged following CCH stimulation, as indicated by the depletion of these vesicles in resting acini exposed to nocodazole or dynamitin overexpression (Fig. 11). Evidence for direct dynein association with these vesicles includes the finding that traces of $p150^{Glued}$ and rab3D labeling are colocalized in resting and CCH-stimulated acini (Fig. 4) and the identification of a small amount of rab3D in peak j (Fig. 7), which contains major stores of dynein and VAMP2. Rab3D-enriched secretory vesicles in lacrimal acini may use small amounts of dynein to maintain their subapical localization by anchoring to MTs. Alternatively, rab3D-enriched vesicles may be formed and dynamically maintained from precursors (similar to VAMP2-enriched transport vesicles) transported by dynein.

The recruitment of dynein and its cargo to the subapical region in response to CCH stimulation suggests that dynein-driven secretory traffic is physiologically regulated through signaling pathways triggered by activation of the M3 muscarinic receptor, the target of CCH action. One potential target of regulation may be the dynactin complex, which exhibits a small but significant increase in its relative abundance in the Tx-100 insoluble, SDS soluble protein pool from CCH-stimulated acini relative to resting acini (Fig. 3). This change in partitioning behavior could reflect association with a new membrane cargo enriched in Tx-100-resistant membranes or alternatively a tighter binding to MTs either alone or in association with membrane cargo. Dynactin recruitment to MTs has previously been proposed as a mechanism for assembly of the holo-complex required for dynein-driven vesicle transport (Vaughan et al., 1999). Interestingly, the content of dynein in the Tx-100 insoluble, SDS soluble protein pool is not increased by CCH in parallel with the dynactin complex. Failure to observe increased dynein in this pool may reflect a more labile association, even in its activated state. Data obtained by dynamitin overexpression are also consistent with the concept that physiological regulation of dynein in acinar secretory traffic may occur through modulation of the dynactin complex. The observation of increased punctate Arp1 fluorescence throughout the cytoplasm of Ad-Dynt-transduced acini stimulated with CCH (Fig. 10), in parallel with the lack of inhibition of CCH-induced recruitment of Arp1 to the SDS-soluble fraction (Table 2), suggest that one mechanism for recruitment of dynactin to membranes may involve regulation of the Arp1 filament.

However, data obtained by fractionation of membranes from resting and CCH-stimulated acini (Figs 6 and 7) also show that although dynein and dynactin are largely associated with the same membranes, their relative abundances vary. The abundance of dynein in higher density regions of the gradient (fractions 11, 12 and P) is relatively greater than that of the dynactin complex. These observations indicate that the factors governing assembly of an active dynein-dynactin holo-complex may be even more complicated than has previously been anticipated.

Growth factors in tears aid in corneal and conjunctival wound healing, whereas bacteriostatic factors (IgA, lactoferrin, lysosomal hydrolases) are essential for ocular clearance of pathogens. Deficiencies in lacrimal acinar protein secretion are associated with a variety of diseases ranging from keratoconjunctivitis sicca to the severe dry eye associated with immune-mediated disorders such as Sjögren's syndrome, AIDS and graft versus host disease. Further exploration of the contributions of dynein and other effectors to stimulated protein release in lacrimal acini may shed insights into the etiology of these processes.

This work was supported by NIH grants EY-11386 to S.H.A., EY-05081 and EY-13720 to A.K.M., a grant from Allergan and by NIH 1 P30 DK48522 (Confocal Microscopy, Subcellular Membrane and Organelle and Viral Vector Subcores, USC Center for Liver Diseases). Additional salary support to S.F.H.-A. was from NIH grants NS38246, DK56040 and GM59297. G.J. received a summer research fellowship from Fight for Sight (Prevent Blindness America). S.R.d.C. was the recipient of an NIH minority predoctoral fellowship (EY-07037). We thank Maria Runnegar and Joel Schechter for helpful discussions and Andrew Stolz for expert assistance with molecular biology constructs.

References

Allan, V. (1996). Motor proteins: a dynamic duo. *Curr. Biol.* **6**, 630-633.
Burkhardt, J. K., Echiverri, C. J., Nilsson, T. and Vallee, R. B. (1997).

Overexpression of the dynamitin (p50) subunit of the dynactin complex disrupts dynein-dependent maintenance of membrane organelle distribution. *J. Cell Biol*. **139**, 469-484.

da Costa, S. R., Yarber, F. A., Zhang, L., Sonee, M. and Hamm-Alvarez, S. F. (1998). Microtubules facilitate the stimulated secretion of β-hexosaminidase in lacrimal acinar cells. *J. Cell Sci.* **111**, 1267-1276.

Dartt, D. A. (1994). Signal transduction and activation of the lacrimal gland. In *Principles and Practice of Ophthalmology*, 2nd edn (ed. D. M. Albert and F. A. Jacobiec), pp. 458-465. Philadelphia: Saunders.

Echiverri, C. J., Paschal, B. M., Vaughan, K. T. and Vallee, R. B. (1996). Molecular characterization of the 50 kD subunit of dynactin reveals functions for the complex in chromosome alignment and spindle organization during mitosis. *J. Cell Biol*. **132**, 617-633.

Fischer von Mollard, G., Stahl, B., Li, C., Sudhof, T. C. and Jahn, R. (1994). Rab proteins in regulated exocytosis. *Trends Biochem. Sci*. **19**, 164-168.

Fujita-Yoshigaka, J., Dohke, Y., Hara-Yokoyama, M., Kamata, Y., Kozaki, S., Furuyama, S. and Sugiya, H. (1996). Vesicle-associated membrane protein 2 is essential for cAMP-regulated exocytosis in rat parotid acinar cells. *J. Biol. Chem.* **271**, 13130-13134.

Fullard, R. (1994). Tear proteins arising from lacrimal tissue. In *Principles and Practice of Ophthalmology*. 2nd edn (ed. D. M. Albert and F. A. Jacobiec), pp. 473-479. Philadelphia: Saunders.

Gaisano, Y. Y., Sheu, L., Foskett, J. K. and Trimble, W. S. (1994). Tetanus toxin light chain cleaves a vesicle-associated membrane protein (VAMP) isoform 2 in rat pancreatic zymogen granules and inhibits enzyme secretion. *J. Biol. Chem.* **269**, 17062-17066.

Gierow, J. P., Yang, T., Bekmezian, A., Liu, N., Norian, J. M., Kim, S. A., Rafisolyman, S., Wood, R. L. and Mircheff, A. K. (1996). Na,K-ATPase in lacrimal gland acinar cell endosomal system. Correcting a case of mistaken identity. *Am. J. Physiol.* **271**, C1685-C1698.

Gill, S. R., Schroer, T. A., Szilak, I., Steuer, E. R., Sheetz, M. P. and Cleveland, D. W. (1991). Dynactin, a conserved, ubiquitously expressed component of an activator of vesicle motility mediated by cytoplasmic dynein. *J. Cell Biol.* **115**, 1639-1650.

Goltz, J. S., Wolkoff, A. W., Novikoff, P. M., Stockert, R. J. and Satir, P. (1992). A role for microtubules in sorting endocytic vesicles in rat hepatocytes. *Proc. Natl. Acad. Sci. USA* **89**, 7026-7030.

Hamm-Alvarez, S. F., da Costa, S. R., Yang, T., Wei, X., Gierow, J. P. and Mircheff, A. K. (1997). Cholinergic stimulation of lacrimal acinar cells promotes redistribution of membrane-associated kinesin and the secretory protein β-hexosaminidase, and activation of soluble kinesin. *Exp. Eye Res.* **64**, 141-156.

Hansen, N. J., Antonin, W. and Edwardson, J. M. (1999). Identification of SNAREs involved in regulated exocytosis in the pancreatic acinar cell. *J. Biol. Chem*. **274**, 22871-22876.

Hirokawa, N. (1998). Kinesin and dynein superfamily proteins and the mechanism of organelle transport. *Science* **279**, 519-526.

Hollenbeck, P. J. (1989). The distribution, abundance and subcellular localization of kinesin. *J. Cell Biol.* **108**, 2335-2342.

Holleran, E. A., Karki, S. and Holzbaur, E. L. F. (1998). The role of the dynactin complex in intracellular motility. *Int. Rev. Cytol.* **182**, 69-109.

Holzbaur, E. L. F. and Vallee, R. B. (1994). Dyneins: molecular structure and cellular function. *Annu. Rev. Cell Biol*. **10**, 339-372.

Mendell, J. R. and Whitaker, J. N. (1978). Immunocytochemical localization studies of myelin basic protein. *J. Cell Biol.* **76**, 502-511.

Mircheff, A. K. (1989). Isolation of plasma membranes from polar cells and tissues: apical/basolateral separation, purity, and function. *Methods Enzymol.* **172**, 18-34.

Ohnishi, H., Ernst, S. A., Wys, N., McNiven, M. and Williams, J. A. (1996). Rab3D localizes to zymogen granules in rat pancreatic acini and other exocrine glands. *Am. J. Physiol.* **271**, G531-G538.

Qian, L., Yang, T., Chen, H. S., Xie, J., Zeng, H., Warren, D. W., MacVeigh, M., Hamm-Alvarez, S. F. and Mircheff, A. K. (2002). Heterotrimeric GTP-binding proteins in the lacrimal acinar cell endomembrane system. *Exp. Eye Res.* **74**, 7-22.

Robin, P., Rossignol, B. and Raymond, M. N. (1995). Effect of microtubule network disturbance by nocodazole and docetaxel (Taxotere) on protein secretion in rat extraorbital lacrimal and parotid glands. *Eur. J. Cell Biol.* **67**, 227-237.

Schafer, D. A., Gill, S. R., Cooper, J. A., Heuser, J. E. and Schroe, T. A. (1994). Ultrastructural analysis of the dynactin complex: an actin-related protein is a component of a filament that resembles F-actin. *J. Cell Biol.* **126**, 403-412.

Schroer, T. A. (1996). Structure and function of dynactin. *Semin. Cell Biol.* **7**, 321-328.

Thurig, L., van Herringen, N. J. and Wijngaards, G. (1984). Comparison of enzymes of tears, lacrimal gland fluid and lacrimal gland tissue in the rat. *Exp. Eye Res.* **38**, 605-609.

Valentijn, J. A., Sengupta, D., Gumkowski, F. D., Tang, L. H., Konieczko, E. M. and Jamieson, J. D. (1996). Rab3D localizes to secretory granules in rat pancreatic acinar cells. *Eur. J. Cell Biol.* **70**, 33-41.

Vaughan, K. T. and Vallee, R. B. (1995). Cytoplasmic dynein binds dynactin through a direct interaction between the intermediate chains and $p150^{Glued}$. *J. Cell Biol*. **131**, 1507-1516.

Vaughan, K. T., Hyman, S. H., Faulkner, N. E., Echeverri, C. J. and Vallee, R. B. (1999). Colocalization of cytoplasmic dynein with dynactin and CLIP-170 at microtubule distal ends. *J. Cell Sci.* **112**, 1437-1447.

Waterman-Storer, C. M., Karki, S. and Holzbaur, E. L. F. (1995). $p150^{Glued}$ binds directly to both the microtubule and centractin. *Proc. Natl. Acad. Sci. USA* **92**, 1634-1638.

Yang, T., Zeng, H., Zhang, J., Okamoto, C. T., Warren, D. W., Wood, R. L., Bachmann, M. and Mircheff, A. K. (1999). Major histocompatibility complex class II molecules, cathepsins B and D, and La/SSB proteins in lacrimal gland acinar cell endomembranes. *Am. J. Physiol*. **277**, C994-C1007.